Design, Manufacturing Status, First Results of the LHC Main Dipole Final Prototypes and Steps towards Series Manufacture

K.Artoos, L.Bottura, P.Fessia, M.Bajko, M.Modena, O.Pagano, D.Perini, F.Savary, W.Scandale, A.Siemko, G.Spigo, E. Todesco, J.Vlogaert, C.Wyss / *CERN, Geneva, Switzerland*

Abstract — **This paper reports about the program of six LHC superconducting main dipole final prototypes and the steps towards series manufacture. The above program, launched in summer 1998, relies on collared coils manufactured by industry and cold masses assembled at the CERN Magnet Assembly Facility. Following design, stability and robustness studies, the magnet design for series manufacture features a "6-block" coil and austenitic steel collars. A general description of the magnet with its main components is given and the main working parameters and the most important manufacturing features are presented. Results of mechanical and magnetic measurements are given as well as the performances of the first prototype. A comparison with results from the previous generation of dipole magnet models and prototypes is also made. Finally an outlook towards series manufacture is given.**

I. Introduction

To validate the major design features selected [1] in view of the series manufacture of the 1232 LHC superconducting (SC) main dipole magnets, CERN has launched in the summer of 1998 the fabrication of 3 x 2 prototype collared coils in industry. These collared coils are subsequently assembled into cold masses at the CERN Magnet Assembly Facility. The first prototype dipole cold mass was tested during the summer of 1999, the assembly of the second one is in progress. It is expected to complete the assembly and testing of the remaining four prototypes by summer 2000. This program also allows to fine-tune assembly procedures and the detail design of ancillary components with a view to minimise assembly time and component costs. The experience and know-how gained will provide the basis for the imminent beginning of the manufacture of 3 x 30 series dipole magnets by industry.

II. Description of the LHC Main Dipole

The dipole magnet cross-section is shown in Fig. 1, while 1-beam tube; 2-SC coils; 3-austenitic steel collars; 4-iron yoke; 5-iron yoke "insert", 6-shrinking cylinder / He II vessel; 7-heat exchanger tube; 8-dipole bus-bars; 9-arc quadrupole and "spool-pieces" bus-bars; 10-wires for magnet protection and instrumentation.

Its main parameters are given in Table I and the main parameters of the SC cables are given in Table II. The design studies which have lead to the selection of the above cross-section for series manufacture are reported in [2] and [3]. The dipole cold mass consists of an active part, providing two

apertures for the cold bore tubes, and of ancillary parts allowing for operation at 1.9 K in superfluid helium. The

Manuscript received on 27 September 1999

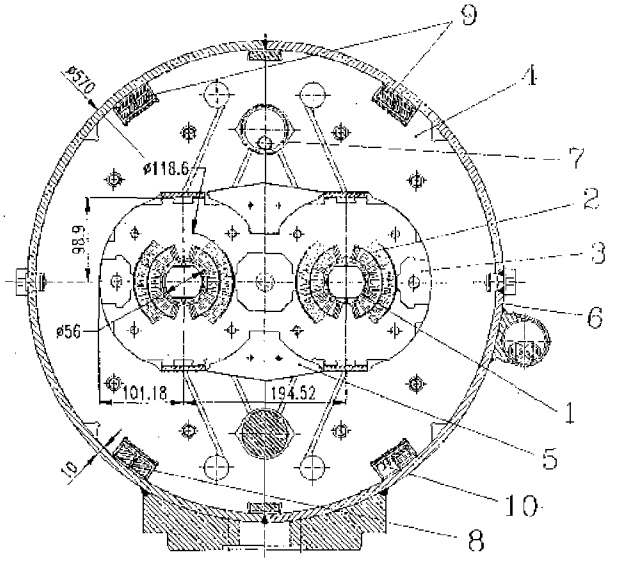

Fig. 1. Cross-section of LHC series dipoles.

active part is made of:

i) Two dipole coils, each consisting of an upper and a lower pole. Each pole consists of an inner and an outer layer, connected in series. The coils are equipped with quench heaters, to trigger a general quench of the layers in case of detection of an initial local quench.

ii) Austenitic steel (AS) fine-blanked collars (3 mm thick), which confines and pre-stresses the coils, so that they strictly maintain their geometry in spite of the very high electromagnetic forces occurring during magnet testing and operation.

Items i) and ii) together with the related cold bore tubes constitute the collared coils.

iii) The 13572-mm long low-carbon iron yoke, made out of 5.8-mm-thick fine-blanked laminations, split in two parts at the vertical symmetry plane. The yoke is completed at both ends, over a length of 513 mm, by AS laminations (3 mm thick) to lower by about 15 % the magnetic field at the coil ends.

iv) Two laminated iron inserts placed across the vertical symmetry plane, completing the magnetic yoke and also constituting the vertical force-carrying element between the collared coils and the yoke.

v) An AS shrinking cylinder, 14760-mm long and at least 10-mm-thick, made up of two longitudinally-welded half-cylinders (the latter manufactured without any welds), surrounding the yoke. For series manufacture, the half-cylinders are bent to achieve, after welding, the horizontal

TABLE I
MAIN PARAMETERS AND CHARACTERISTICS OF THE DIPOLE COLD MASS

	Value	Unit
Inj. field (0.45 TeV beam energy)	0.54	T
Nom. field (7 TeV beam energy)	8.33	T
Nominal current	11 800	A
Operating temperature	1.9	K
Magnetic length at 1.9 K	14.300	m
Nom. stored energy (two bores)	7.1	MJ
Ultimate operational field	9.00	T
Nominal short sample field limit	9.65	T
Apertures axis distance at 1.9 K	194.00	mm
Bending radius at 1.9 K	2803	m
Aperture axis distance at 293 K	194.52	mm
Approx. bending radius at 293 K	2812	m
Inner coil diameter at 293 K	56.00	mm
Outer coil diameter at 293 K	118.60	mm
Conductor blocks / pole	6	
Turns / pole, inner/outer layer	15/25	
E.m. forces/coil quadrant at 8.3 T		
Hor. force (inner and outer layer)	1.7	MN/m
Vertical force (inner layer)	-0.14	MN/m
Vertical force (outer layer)	-0.60	MN/m
Axial electromag. force on both ends at nom. field	0.37	MN
Cold bore inner/outer diameter at 293 K	50/53	mm
Active part length at 293 K	15 180	mm
Cold mass diameter at 293 K	570.0	mm
Overall length with ancillaries	16.8	m
Mass of the cold mass	~ 30	tonne

TABLE II
MAIN PARAMETERS OF THE SC CABLES

	Inner layer	Outer layer	Unit
Strand diameter	1.065	0.825	mm
Strand Cu/SC ratio	1.65	1.95	mm
Filament diameter	7	6	μm
Filaments / strand	8800	6400	
Number of strands	28	36	
Ic at 1.9 K and 10 T	13750		A
Ic at 1.9 K and 9 T		12960	A
Cable width	15.1	15.1	mm
Keystone angle	1.25	0.9	deg
Cable mid-thickness	1.90	1.48	mm
Transposition pitch	115	100	mm

curvature of the cold mass. The shrinking cylinder gives to the cold mass assembly the stiffness necessary to contain the electromagnetic forces, provides the inertia necessary to maintain to within ± 1 mm the geometry of the cold mass on its supports, and is the major part of the helium containment vessel. In its latter function, it must be able to resist to pressures up to 2 MPa which may occur during a quench.

vi) Two 50-mm-thick AS end plates, terminating the active part at both extremities, to take up the longitudinal electromagnetic forces.

III. MANUFACTURE OF PROTOTYPE COILS

The manufacture of prototype collared coils has been entrusted to three European firms (Ansaldo, Alstom-Jeumont and Noell). The coils have an overall length of 14567 mm; the difference between the average azimuthal size and its actual value at any point along layers and poles, measured under a 50 MPa compressive load, must not exceed ± 25 μm. For the inner and outer layer, SC cable lengths of 460 m and 750 m are required, respectively. To run-in tooling like winding mandrels, curing molds and the various manufacturing operations, dummy coils wound with copper cables were made first.

In all the prototype coils the inner and outer layers are joined (SnAg4.5 soldering alloy, joint resistance < 1 nΩ at 1.9 K) immediately after the inner layer ramp. The joined cables are locked in a charged ULTEM* box designed to position both the ramp and splice.

The coil production at the three different sites is fulfilling the necessary and required precision and reproducibility. Two manufacturers have produced coils within the tolerance range of ± 25 μm on the transverse dimensions. A third manufacturer is at present solving a tooling problem causing in the first layer a precision of ± 100 μm. The good reproducibility is evidenced by the fact that the collaring shims used for the different poles are within ± 0.05 mm. This evaluation of reproducibility and precision takes also into account the small difference between the SC cables delivered to the coil manufacturers (cables from different suppliers are used for the prototype coils) and the characteristics of the major tooling (i.e. winding machines, curing molds and curing presses) presently available at the different sites.

Following the imminent start of the work for the manufacture of 3 x 30 cold masses, the still missing main tooling is being procured by the firms and will be available in the first half of next year.

IV. COIL COLLARING

One of the main results expected from the assembly of the prototypes is the optimisation of the pre-collaring and collaring procedures. During pre-collaring the collars are kept around the coils by locking rods of a diameter smaller by 1 mm than nominal; during collaring the nominal rods are inserted. The presses foreseen for the series production will allow to insert the three nominal locking rods in a single operation. Two such presses are already operational at Ansaldo and Alstom-Jeumont, a third one is being procured by Noell.

Consequently, the recent collaring at Noell of prototypes MBP2N1 (AA** collars) and MBP2N2 (AS collars) was made in two steps (application of pressure first on the collar sides and insertion of the side rods, followed by application of pressure at the collar centre and insertion of the central rod). During pre-collaring an expansible mandrel was used to push radially the coils against the collar cavity. Subsequently, the mandrel is removed and the cold bore tube is inserted.

In order to minimise assembly time, simpler procedures will be tested at Alstom and at Ansaldo (pre-collaring with the cold bore tube already inserted). The azimuthal coil pre-stress after collaring in the coil straight part of MBP2N1 and MBP2N2 is reported in Table III.

* ULTEM is a trademark of General Electric, USA.
** Aluminium alloy

TABLE III
AVERAGE PRE-STRESS AFTER COLLARING IN THE STRAIGHT SECTIONS OF THE MBP2N1 AND MBP2N2 COLLARED COILS

	MBP2N1 (AA collars)	MBP2N2 (AS collars)
Inner layer	45 MPa	65 MPa
Outer layer	45 MPa	70 MPa

The pre-stress distribution in the ends of MBP2N1 is not well known due to the poor Young modulus measuring system then available. The measurement quality was largely improved for MBP2N2, where a pre-stress distribution in the coil ends following the law $\sigma(x) = 30 + (\sigma_0 - 30)(1 - tg(\pi/4 \cdot x/180))$ where σ_0 is the pre-stress in the straight part and x is the distance from the end of the straight part. Distances are in millimetres and stresses in MPa. Further input concerning the optimisation of the coil end pre-stress is being provided by the short model programme [4].

V. COLD MASS ASSEMBLY

The dipole cross-section design shown in Fig. 1 has allowed a much easier and faster assembly of collared coils and iron half-yokes than the previous design [5]. The latter relied on a vertical interference of 0.14 mm between collars and yoke (to compensate for the reduction in vertical size of the collared coils at high field, because of the unloading by electromagnetic forces of the coil pre-stress) and on a nominal yoke vertical gap of 0.52 ± 0.05 mm after longitudinal welding of the shrinking cylinder. The first condition required tedious measurements and adjustments because of the spread in collared coil height, caused by the fitting of the magnetic insert into the AA collars. The second condition required tight tolerances on the half circumference of the shrinking cylinder half-shells and a very precise control of the welding shrinkage.

The first prototype (MBP2N1) of the present series of six was still equipped with aluminium collars and its yoke was assembled with laminations of non-nominal geometry, left from previous work, because of availability. Collars and yoke had however a geometry close to that shown in Fig.1. The collared coils and the iron inserts kept together by a fixture could be inserted without any difficulties in the yoke. After welding, the average azimuthal pre-stress in the shrinking cylinder was 180 MPa and the average yoke gap between the yoke-halves was 0.2 mm.

The second prototype (MBP2N2) is equipped with AS collars, as per final design. For welding, a vertical load of about 660 tonnes per metre length was applied. In this case, the half-yokes are acting as a mechanical stop and it is no longer necessary to control the gap closure during the assembly and welding operations as it was the case in the past. Therefore, the tolerances on the half-circumference of the shrinking cylinder shells can be increased from 0.1 mm to 0.5 mm, considerably easing their series production. After MAG welding, a residual gap of 0.05 mm was observed; a larger weld contraction will be set for the next prototype.

Later during assembly, an axial load is applied on the coil-heads to provide a support against the axial component of the electromagnetic forces occurring in operation. More details about this subject are given in [6].

The 3-D measurements, based on laser tracker technology, of the MBP2N1 cold mass geometry showed that horizontal curvature and vertical straightness [1] were achieved within ± 1 mm, as required. The measurement of the MBP2N2 cold mass geometry is imminent.

VI. TEST RESULTS

A. *Field Quality Measurements at Room Temperature*

The field-shape components of the MBP2N1 cold mass were measured at room temperature, prior to the power tests at 1.9 K, with a excitation current of 20 A [7]. The results are given in Table IV, in units of 10^{-4} at a reference radius R_{ref} = 17 mm. They are compared to the expected values, computed for the nominal coil and hybrid yoke geometry.

The components measured in Aperture 2 differ by less that 10 %, from those of Aperture 1. The differences between the measured and the expected values of the low order harmonics, with the exception of b_4 and b_9, are within the allowed R.M.S. variation. These differences are most likely induced by imperfections of the coil geometry. The high b_2 and b_4 values are a feature of the particular yoke of MBP2N1. The b_2 value of the nominal design is 0.32 units. The high value of b_9 is not yet explained and will be investigated. The magnetic measurements at room temperature were repeated after the power tests. The values of the field-shape harmonics were found to be stable within 6%. This indicates that the coil geometry is stable to within random movements, see [8] for a detailed analysis. The results relative to the previous five-blocks coil design were rather different [9]. The stability of the coil was much weaker. The initial powering and thermal cycle produced a systematic movement of 50 μm of the large angle blocks of the inner coil layer in the radial outward direction.

B. *Power Test*

The power test campaign of the MBP2N1 prototype started in March 1999 and was divided into several runs separated by a thermal cycle from 1.9 K to room temperature and back to 1.9 K. Up to now the magnet was quenched at 1.9 K in total 57 times. The complete training quench history is shown in Fig.2.

TABLE IV
MBP2N1 COLD MASS, FIELD SHAPE COMPONENTS AT ROOM TEMPERATURE AND AT I = 20 A, MEASURED PRIOR TO THE POWER TESTS. UNITS OF 10^{-4} AT A REFERENCE RADIUS R = 17 MM

n	Computed harmonics		Measured harmonics (Aperture 1)	
	normal	skew	normal	skew
2	4.25	-	5.48	1.00
3	7.32	-	8.10	-0.38
4	0.00	-	0.66	0.06
5	-1.05	-	-0.69	-0.07
6	0.00	-	-0.20	0.02
7	0.63	-	0.57	0.02
8	0.00	-	-0.30	0.01
9	0.10	-	0.25	-0.02

During the tests the magnet was protected against quench induced damage by means of quench heaters and additionally by energy extraction to an external dump resistor. Usually 10% to 20% of the total stored energy was extracted. In the first test run the magnet was cooled maintaining from 293 K to 80 K a longitudinal temperature gradient of about 5 K/m. The first natural quench occurred at 7.35 T and after two more training quenches the nominal field of 8.33 T was exceeded. At the tenth quench, the magnet reached 8.9 T, the highest value of the first run. Subsequently, a fast thermal cycle (direct injection of helium gas at 80 K) was performed. The aim of the second run was to observe up to which field level the magnet kept a memory of the previous training and whether the fast thermal cycle had an influence on quench behaviour. In this run, the first quench occurred at 8.4 T (a 1.1 T gain with respect to the first run, corresponding to 66% of the 1.6 T increase achieved in the first run training), the highest field was 9.2 T at the sixteenth quench. All the 15 training quenches of the first run and 18 quenches out of 20 of the second run were located in the transition regions of the coil ends. For the first run, quenches were located mainly in the non-connection end (NCE), while for the second run they were mainly in the connection end (CE), submitted to high axial load and thermal stress during the fast cool down. Two quenches, at 8.75 T and 9.2 T, occurred in the coil straight sections, during the second run only. The observed quench locations and the high axial forces measured [6] lead to the decision to remove the magnet end-covers and reduce from 50 to 10 kN/aperture the design coil pre-compression at room temperature. After the above mechanical intervention, the third run consisted of only one quench (at NCE) at a field of 7.9 T. For this quench an exceptionally high quench load of 43 MA^2 (instead of about 30 MA^2) was recorded. The resulting hot spot temperature and voltages across hot parts of the coil exceeded by far the values that were observed during the previous quenches. The hottest spot temperature was evaluated to be about 800 K, assuming adiabatic conditions.
An analysis of the data showed that the quench detection and the energy extraction systems were working correctly, but that the current pulse delivered by the quench heater power supplies was abnormal and did not reach the heater strips.

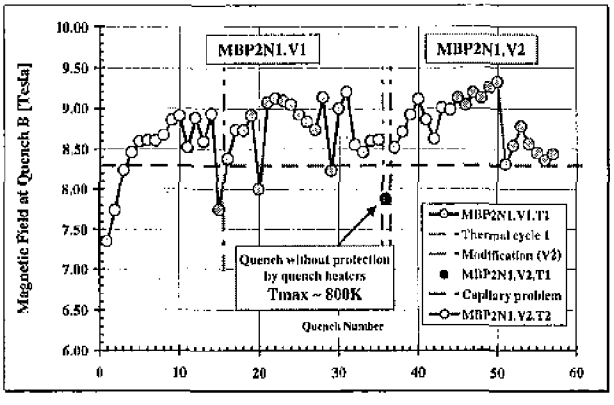

Fig. 2. MBP2N1 prototype, history of the training quenches

Only the energy extraction system protected the magnet. In fact, the heater strips were not activated because of a voltage breakdown between connector pins in the warm connection box on top of the cryostat. After repair, the magnet was cooled down and the test resumed. The first quench occurred at 8.5 T, 9 T was exceed after the third one and the new maximum field of 9.3 T was reached at the fourteenth quench. The above performance proved the robustness of the magnet structure and its ability to withstand accidental excessive local overheating and over-voltage without any impact on quench behaviour. The quench locations were very similar to those observed during the first two runs, with the first 13 quenches at NCE and the following eight ones at CE.

In conclusion, the magnet was able to exceed nominal field after three training quenches, and after thermal cycles the first quench was above nominal field. The coil end regions are limited above ultimate field (9 T), beyond which mechanical instabilities are triggered, leading to subsequent lower quench fields. The coil straight parts behaved reasonably well, showing only the two previously quoted quenches throughout the four power test runs.

C. *Cold Field Quality Measurements*

Table V reports the main results of the magnetic measurements performed in cold conditions. We report there values of the harmonics measured at injection field (0.54 T) and at nominal field (8.3 T) and integrated over the magnet length. We note first that the harmonics at high field agree reasonably well with the results of warm measurements. The sextupole, decapole and 14-pole, allowed by symmetry, are close to the values measured in warm conditions. The significant difference in the normal quadrupole can be partially explained by the effect of iron saturation (2.5 units). The comparison of the values at injection and at high field show that the partial compensation of the persistent current contribution by means of a geometric offset on the allowed normal sextupole, decapole and 14-pole is very effective. Indeed the magnet has a better overall field quality at injection, where the beam requirements are more strict, than at high field. Finally in Fig. 3 we report the evolution of the geometric sextupole (evaluated at 5 kA) throughout the powering of the first test campaign. We see that the magnet is geometrically very stable, as already shown by the results of the warm measurements before and after the test. Overall the change of normsextupole was below 0.15 units at 17 mm. This is three times better than in a previous 15-m long prototype, MBP1A1 also shown in Fig. 3, with a 5 block coil geometry.

VII. Schedule for the Remaining Prototypes

The next four collared coils will be delivered from industry from mid October to end December 1999 so that the remaining cold mass assemblies will be tested by mid 2000. This programme, carried out in collaboration with industry is thus overlapping with the expected beginning of series manufacture.

TABLE V
HARMONICS IN COLD CONDITIONS, AT INJECTION (0.54 T) AND HIGH FIELD (8.3 T) UNITS OF 10^{-4} AT A REFERENCE RADIUS R = 17 MM

	Injection				High field			
n	Aperture 1		Aperture 2		Aperture 1		Aperture 2	
	normal	skew	normal	skew	normal	skew	normal	skew
2	1.03	0.70	-2.27	0.50	-1.47	1.69	1.17	1.52
3	-0.76	0.08	-0.27	-0.30	6.34	0.12	6.97	-0.12
4	0.32	0.09	-0.44	0.04	0.01	-0.19	-0.13	-0.21
5	-0.05	0.06	0.21	0.04	-0.97	0.13	-0.93	0.08
6	0.04	0.00	-0.02	0.01	0.01	0.21	-0.04	0.22
7	0.16	-0.02	0.20	-0.03	0.52	0.02	0.57	0.03
8	0.02	0.05	-0.01	0.04	0.02	0.05	0.00	0.05
9	0.26	-0.04	0.28	-0.04	0.03	-0.03	0.04	-0.02

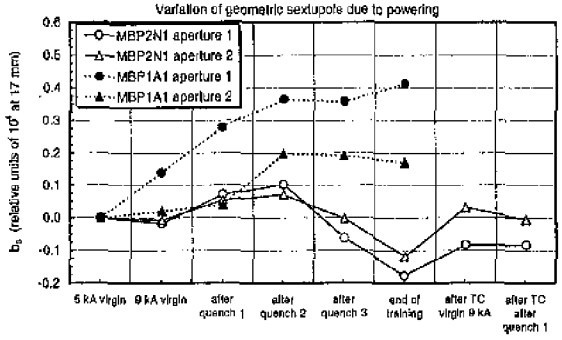

Fig. 3. Evolution of the geometric sextupole of MBP2N1 throughout the first powering campaign, compared to the sextupole changes measured on the MBP1A1 prototype.

VIII. STEPS TOWARDS SERIES MANUFACTURE

Following a call for tenders issued in December 1998 and the approval by the CERN Finance Committee in June 1999 of the contract adjudication proposals, the start of activities at the previously quoted three firms for the manufacture of 3 x 30 dipole cold masses is imminent. The aim is to establish the industrial learning curve for dipole cold mass series manufacture, and to issue in the year 2001 the call for tenders for the remaining 1168 units.

Concerning the procurement of SC cables, the corresponding contracts were placed in the course of 1998. For the dipole inner (cable 1) and outer (cable 2) layers, about 3906 km of "Cable 1" and 3740 km of "Cable 2" are required, respectively. The supply of Cable 1 is entrusted to two European firms, that of Cable 2 also to two European firms for a total of 3320 km* and to one US and one Japanese firm, each for a length of 504 km*. The SC pilot strand production has started, by end of 1999 it is expected to reception the first cable lengths from the pilot cable production (1 % of the total length).

* Main Dipoles and Quadrupoles

IX. CONCLUSION

The series design for the LHC dipole magnets is being validated this year with the manufacture and testing of a set of six full-length prototypes, the last of which will be cold tested by the end of spring 2000. The performance of the first prototype, of a design close to the series one, is fulfilling the specifications required for LHC operation at the nominal field of 8.3 T. Its performance is limited above the ultimate field of 9 T by the coil end regions. Design and experimental work is in progress to fully understand this limit and push it towards higher field levels. The field quality of the first prototype is rather satisfactory and its geometry is within specifiction.

Industrial production of SC cables has begun, the start of the manufacture by industry of 90 dipole cold masses is imminent. The call for tenders for the manufacture of the 1142 remaining cold masses is scheduled for the year 2001.

ACKNOWLEDGMENTS

The work described here is the result of the ingenuity, professional competence, enthusiasm, untiring efforts of a large number of colleagues in the LHC and EST divisions, and of the firm and inspiring support of L.Evans.

REFERENCES

[1] C.Wyss,"LHC arc dipole status report", PAC99, New York
[2] P.Fessia et al, "Selection of the cross-section design for the LHC main dipole", this Conference
[3] M.Bajko, P.Fessia, D.Perini, "Statistical studies of the robustness of the LHC main dipole mechanical structure", this Conference
[4] K. Artoos et al, "Status of the short dipole model program for the LHC", this Conference
[5] J.Billan et al, "Test results on the long models and full scale prototype of the second generation LHC arc dipoles", ASC'98, Palm Spring, CA, USA
[6] K.Artoos etal,"Measurement and analysis of axial end forces in a full length prototype of the LHC main dipole magnets", this Conference
[7] S.Gleis et al.,"Analysis of the warm magnetic measurements in a LHC main dipole prototype", this Conference
[8] W. Scandale et al.," Influence of mechanical tolerances on field quality in the LHC main dipole", this Conference
[9] O. Pagano et al, LHC Project Note 180, 1999